Structure and Physical Properties Study of Some Oxide Glasses Used as γ- Ray Shielding Material

H.A. Saudi[1], A. Abd-Elalim[2], T.Z. Abou-Elnasr[2], A.G. Mostafa[2]*

[1.] Phys. Dept., Faculty of Science (Girls' Branch) Al-Azhar University, Nasr City, 11884, Cairo, Egypt
[2.] Phys. Dept., Faculty of Science, Al-Azhar University, Nasr City, 11884, Cairo, Egypt
*drahmedgamal@yahoo.com

Abstract: Some sodium-iron-phosphate glasses containing various amounts of calcium, strontium or barium oxides have been prepared by the melt quenching technique. The amorphous nature has been confirmed by using XRD, while the internal structural groups have been investigated by IR analysis. The studied physical properties indicated that the samples containing 15 mol% BaO represented the highest density and molar volume values among all the studied glasses. It exhibits also the highest mass attenuation coefficient and the lowest half value layer. Although the glass containing 15 mol % CaO exhibits the highest values of both hardness and aqueous durability, but those containing SrO or BaO exhibit also an excellent level of hardness and durability.
[Saudi HA, Abd-Elaleem A, Abou-Elnasr TZ, Mostafa AG. **Structure and Physical Properties Study of Some Oxide Glasses Used as γ- Ray Shielding Material.** *Nat Sci* 2015;13(11):139-145]. (ISSN: 1545-0740). http://www.sciencepub.net/nature. 19. doi:10.7537/marsnsj131115.19.

Keywords: IR Spectroscopy, Mass Attenuation Coefficient, Gamma Ray Shielding Glass, Aqueous Durability, .Hardness

1. Introduction

Recently, some novel compositions based phosphate glasses have been developed where they appeared to be of superior physical and chemical properties [1 - 5]. These glasses are characterized by their high thermal expansion coefficients [6], low melting and softening temperatures, as well as high ultra-violet and far infrared transmission [7, 8]. These interesting properties make phosphate glasses to be of potential candidates for many technological applications as sealing materials, medical use [9] and solid state electrolytes [10].

Among all compositions iron phosphate glasses are usually considered for a variety of applications, where it can be used as semiconductor material and for manufacturing rechargeable batteries as well as memory storage [11]. These glasses are also important in optical technology such as high energy laser application as well as fiber and optical lenses [12, 13]. It was found also that iron phosphate glasses containing some heavy metal oxides have high γ- ray absorption coefficient and accordingly these glasses can be used as γ- ray shielding materials in addition to vitrifying or encapsulating radioactive wastes [14- 17].

Therefore, in this article, some iron sodium phosphate glasses doped with calcium, strontium or barium oxides will be thoroughly investigated by applying XRD and IR spectroscopy to obtain information about their internal structure. Some physical properties will be also studied to achieve the best glasses that can be used as γ- ray shielding and to capsulate the radioactive wastes. Some other related properties as density, molar volume, durability and hardness will be also measured.

2. Experimental Procedure

In this work, three glass systems have been prepared, having the following composition, [(70 - x) mol % P_2O_5 .15 mol % Fe_2O_3. 15 mol % Na_2O. x mol % YO], Where x = 0, 5, 10 or 15 and Y represents Ca, Sr or Ba cations. The weighted batches were ground well in an agate mortar and were then melted in porcelain crucibles for an hour in an electric muffle furnace at 1100 ^oC. The melts were stirred several times to ensure complete homogeneity and were then poured as quickly as possible onto a copper plate at room temperature and were suddenly pressed by a similar plate. The visual examination of the obtained solid glasses exhibited easily their transparence character [18].

X-ray diffraction (XRD) patterns of all samples were obtained using Bruker D8 advanced x-ray diffractometer with an interval and scanning rate of 0.02° and 5° min^{-1} respectively. Cu K_α radiation (λ = 0.1541 nm) was used with tube voltage and current equals 50 kV and 300 mA respectively.

The IR spectra of the studied glasses were obtained, using FTIR- Berken Elmer spectrometer; model RTX, in the range from 4000 to 400 cm^{-1}, applying KBr disk technique.

The experimental density values (ρ_{exp}) were measured applying Archimedes method using toluene as an immersion liquid and the empirical densities (ρ_{emp}) of the corresponding close packed structural compounds were also calculated. The experimental

and empirical molar volume (V_m) values were then calculated. [19, 20].

The values of the total mass attenuation coefficients of the studied glasses were calculated using Win X-COM program, based on the mixture rule and the half value layers *HVL* were also calculated [21-23].

The micro-hardness measurements were carried out using Vickers Micro Hardness indentation tester (HV – 1000 - China). The indentation was made using a square based pyramidal diamond with face angle 136°, measuring microscope and video monitor. The hardness was calculated applying the following equation,

$$H_v = A\ (P/d^2) \qquad kg / mm^2$$

where A is a constant equal to 1854.4, P is the indentation load applied and d the mean value of the indentation diagonal. Five indentations were done, using polished glass samples, with a constant load of 200 g during 20 S for each sample and the mean value was then calculated to be the correct hardness value of the glass under study [24].

For durability measurements, the prepared glasses were polished to obtain disk shape specimens with 1 cm diameter and 1 mm thickness. The dikes were then cleaned with acetone and distilled water, dried and weighted before they immersed in beakers containing 100 ml of underground water. The beakers were placed in an oven at 90˚C for 6, 12, 24 and 48h. The specimens were removed, rinsed with distilled water, dried, and weighted again. The dissolution rate (DR) was calculated from the measured weight losses (Δw) using the following equation [25].

$$DR = \Delta w\ (g) / [\ A\ (cm^2) \times t\ (min)\ ]$$

where A is the total surface area of the sample and t is the immersion time in mints.

3. Result and Discussion

3.1. X-Ray Diffraction

XRD was performed here to confirm the amorphous nature of the studied samples. Fig (1) represents the obtained XRD patterns of the glass samples containing 15 mol % CaO, SrO or BaO, as representative patterns. Broad humps around 2θ = 29 degree have been observed with no indication of any diffraction peaks in all samples. Accordingly, it can be stated that, all glasses exhibit the amorphous nature and the short range order character [26].

3.2. Infrared Analysis

Fig. (2) shows the obtained IR spectra in the range from 400 to 4000 cm^{-1} for the glasses containing 15 mol % of CaO, SrO or BaO, as representative IR spectra.

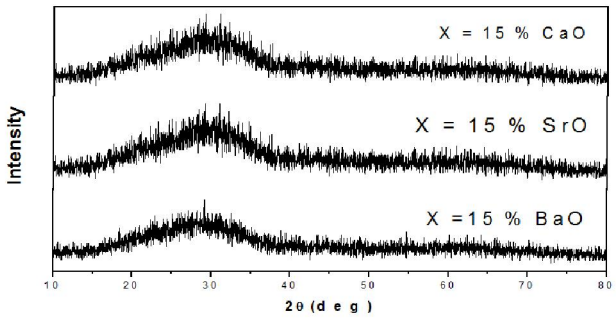

Figure 1. XRD patterns of the glasses containing 15 mol % CaO, SrO or BaO, as representative patterns.

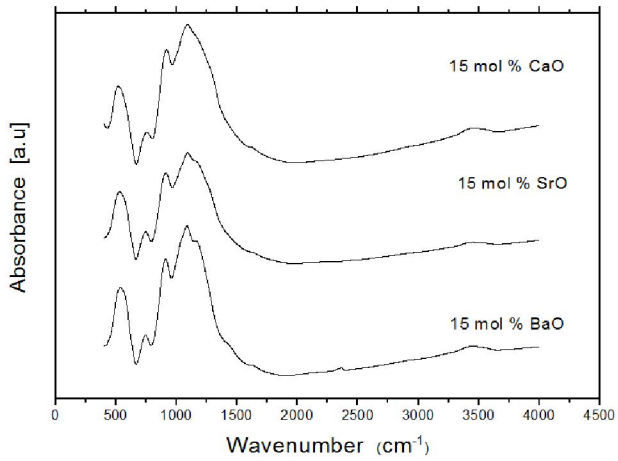

Figure 2. IR spectra of the glasses containing 15 mol % CaO, SrO or BaO, as representative IR spectra.

From this figure, it appeared that many IR absorption bands can be easily observed in the range from 400 up to 1600 cm^{-1}. These bands can be attributed to the vibration of some structural groups and/or some bond vibrations in the glass networks, which can be discussed as follows:

1- The band appeared around 500 cm^{-1} can be assigned to the presence of Fe-O bonds in FeO_6 octahedral symmetry [27].

2- The band appeared in the range from 740 to 770 cm^{-1} can be attributed to the symmetric stretching vibration of P-O-P bond in Q^1 speeches [28].

3- The band appeared between 910 and 920 cm^{-1}, can be assigned to the asymmetric stretching vibration of P-O-P bond in Q^1 speeches [29].

4- The band appeared in the range from 1080 to 1092 cm^{-1}, can be assigned to the vibration of PO_2 and/or $(P-O)^-$ groups in Q^o speeches [30].

5- The band appeared in the range from 1230 to 1250 cm^{-1}, can be correlated to the symmetric stretching vibration of two non-bridging oxygen

atoms bonded to one phosphorus atom in PO_2 unit and / or O=P in Q^2 units [31].

6- The band appeared around 1600 cm^{-1} may be due to the bending vibration mode of –OH group. Also, all spectra show some bands in the ranges from 3440 to 4000 and 2290 to 2380 cm^{-1}. These bands can be attributed to the stretching vibration of – OH groups. The presence of – OH and H-O-H groups may be due the used KBr technique [32, 33].

According to the above survey about IR results, it can be stated generally that the present iron cations occupy mostly the octahedral symmetry, that is iron cations occupy the glass network modifier positions. Phosphates occupy different Q^n speeches which indicated the presence of some non-bridging oxygens.

It can be observed that the band appeared in the range from 1230 to 1250 cm^{-1} (as a shoulder) shows a gradual decrease in its intensity as CaO, SrO or BaO were gradually increased. This behavior may be taken as evidence to the gradual decrease of the P=O groups in the glass networks [32].

3.3. Density and Molar Volume

The densities of the prepared glasses were measured experimentally applying the liquid displacement technique and the obtained values were compared with those obtained theoretically for the close packed structure of the corresponding compounds. Both the experimental and empirical density values of the glass system containing CaO are plotted in Fig. (3). It is seen that both density values (empirical and experimental) increased gradually and linearly with the gradual increases of CaO content. It is observed also that the empirical density is usually higher than the corresponding experimental values [34]. It is worth to state that all systems exhibit similar behavior.

Fig. (4) shows the experimental and empirical density for the glasses containing 15 mol % of CaO, SrO or BaO for comparison. It is observed that the glass containing 15 mol % CaO exhibits the smallest density value while that containing 15 mol % BaO exhibits the highest density value. This may be due to the differences in the atomic weights that decreased in the order Ba > Sr > Ca.

It is suitable to consider the molar volume (V_m) values of the studied glasses since it related directly to the spatial structure of a material. Fig. (5) exhibits the change of the V_m values (experimental and empirical) for the glass system containing different CaO content, as a representative figure. From this figure, it appeared that both the experimental and empirical V_m values show linear gradual decrease with the increase of the introduced CaO, and the empirical values appeared usually lower than those obtained experimentally, and all the studied glass systems show similar behavior. The higher empirical density as well as the lower empirical V_m in comparison to the corresponding experimentally obtained values can be taken as evidence for the amorphous nature and the glassy state character of the studied samples [35].

Fig. (6) shows the experimental and empirical V_m values for the glasses containing 15 mol % CaO, SrO or BaO for comparison. It is appeared that both the experimental and empirical V_m values increased gradually on going from CaO to BaO. This can be attributed to the cationic radius of the introduced cations which take the order Ba > Sr > Ca [36].

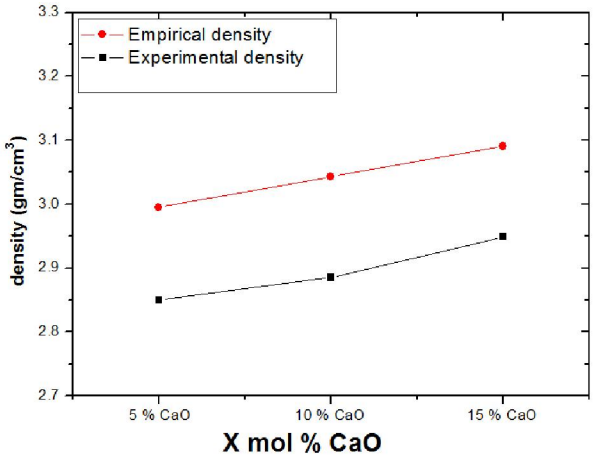

Figure 3. Experimental and empirical density values for the glass system containing CaO, as a representative figure.

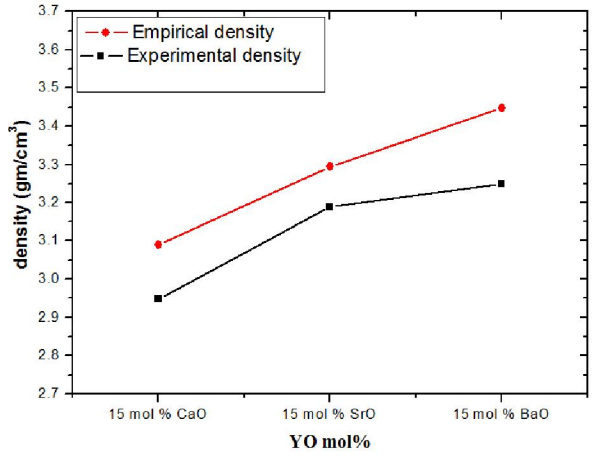

Figure 4. Experimental and Empirical density values of the glasses containing 15 mol % CaO, SrO or BaO for comparison.

3.4. Mass Attenuation coefficient

The attenuation coefficients of the prepared glasses have been also examined in order to check the

ability of these glasses to act as shields from the harmful radiations. However, the γ-ray mass

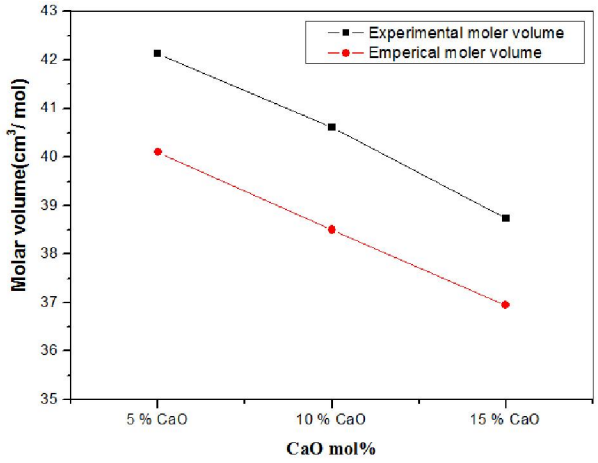

Figure 5. Experimental and empirical V_m values of the glass system containing CaO, as a representative figure.

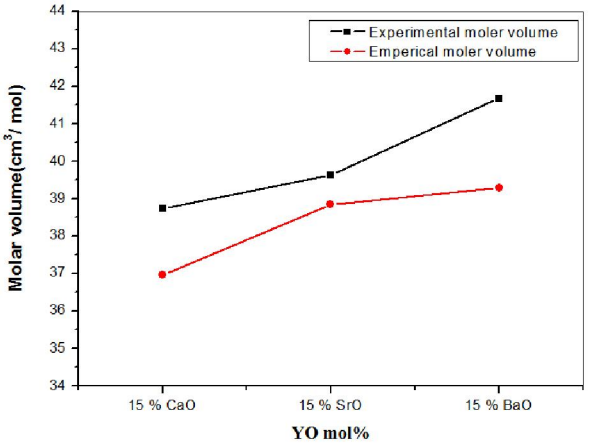

Figure 6. Experimental and empirical V_m values for the glasses containing 15 mol % CaO, SrO or BaO, as a representative figure.

attenuation coefficients (μ/ρ) of the studied glass have been calculated using Win X-COM program at energies equal to 356 KeV (^{135}Ba), 662 & 1173 KeV (^{60}Co) and 1332 KeV (^{137}Cs) as low energy γ-ray and at energies equal to 20, 40, 60 and 80 MeV as high energy γ-ray. Fig. (7) shows the change in the γ-ray mass attenuation coefficient with the gradual increases of CaO oxide at the expense of phosphorus pentoxide, as a representative figure. A gradual increase of the mass attenuation coefficient for low energy γ-ray can be easily observed. The onset drown inside this figure shows obviously the observed increase. Similarly, Fig. (8) represents the change in the mass attenuation coefficient for the glass system containing CaO, as a representative figure. It is observed that both the other glass systems (those containing SrO or BaO) show similar behavior. It appeared that as Ca, Sr or Ba oxides were gradually increased, the mass attenuation coefficient increased. It is also seen that the attenuation effects of all glasses are usually high for low energy γ-ray than those obtained for high energy γ-ray, and the highest γ-ray coefficient is represented by the sample containing 15 mol % BaO. Therefore, it can be stated that these glasses (specially hat contain 15 mol % BaO) can be used preferably as a good shielding material at low energy rays.

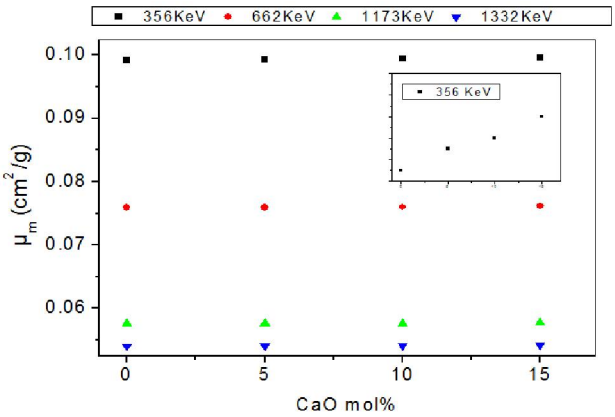

Figure 7. The change of the mass attenuation coefficient versus CaO content for different low γ-ray energies, as a representative figure.

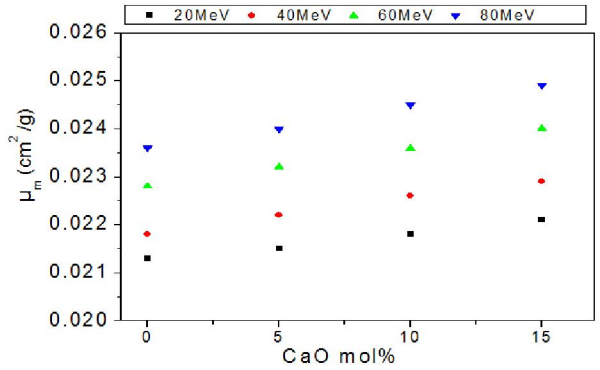

Figure 8. The change of the mass attenuation coefficient as function of CaO content for different high γ-ray energies, as a representative figure.

The half value layer (*HVL*) of the studied glasses was also calculated for the same γ-ray energy values. The obtained values as a function of CaO are represented in Figs. (9 & 10) for low and high energy γ-ray, respectively, as representative figures. It is observed also that, both other systems (those containing SrO or BaO) show similar behavior. It can be seen obviously that the HVL decreased gradually with the gradual increase of Ca, Sr or Ba oxides concentrations. It can be seen that the lowest

HVL is exhibited by the sample containing 15 mol % BaO at low gamma energy and this confirm that this sample is the best shielding material among all the studied glasses.

The observed increase in the γ-ray mass attenuation coefficient as well as the corresponding decrease in the half value layer of the studied glasses can be attributed to the gradual replacement of phosphors oxide by CaO, SrO or BaO. This in turn can be understood knowing that the atomic number (Z) of the introduced cations increased in the order Ba > Sr > Ca [37, 38].

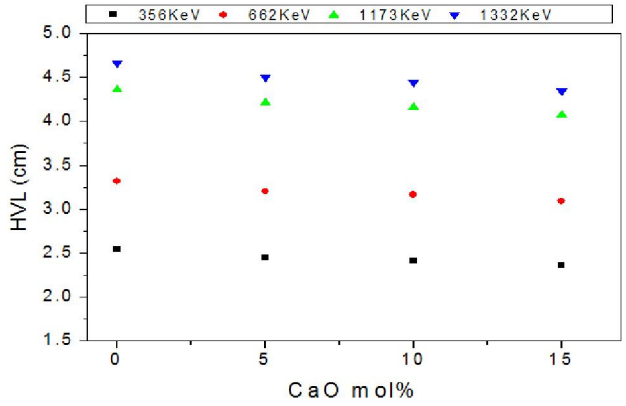

Figure 9. The change of the HVL of the investigated glasses versus CaO content for different low γ-ray energies, as a representative figure.

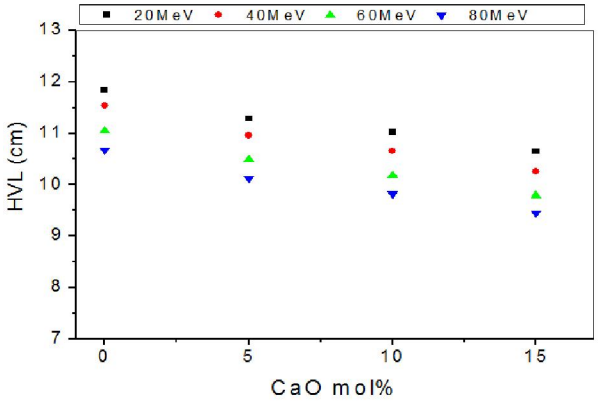

Figure 10. The change of the HVL of the investigated glasses versus CaO content for different high γ-ray energies, as a representative figure.

From the above results about gamma ray attenuation coefficients and *HVL* it can be supposed that all the studied glasses can be used as transparent shielding material and for encapsulating radioactive wastes before interment underground. But, the related properties such as, hardness and chemical durability must be also investigated, since the higher the hardness, the higher is the probability to bear the above load when interment underground, while the higher durability, the higher is its resistance to underground water.

3.5. Dissolution Rate and Durability

The aqueous durability of the studied glasses was checked against underground water at 90°C for different periods (6, 12, 24 and 48 h) in order to obtain information about their chemical and physical stability when interment underground [37]. The dissolution rates (DR) of all glasses were measured and their durability values were then calculated. Tables (1, 2 & 3) represent the logarithm of the dissolution rates as a function of CaO, SrO or BaO respectively. It can be seen from these tables that, DR of the studied glasses is found in the order of $\sim 10^{-1}$ g/cm^2 min, except the glass samples containing15mol% Cao,Sro,or BaO where their DR values are found in the order of $\sim 10^{-2}$ g/cm^2 min. However, these glasses can be considered as chemically durable materials, since it is known that. low DR means high durabilty [39].

It can be observed that the addition of barium, strontium or calcium oxides to iron phosphate glasses improved their durability. All the studied glasses exhibit well to excellent aqueous durability especially those containing 15 mol % of the introduced oxides (CaO, SrO, BaO). They have relatively lower DR and hence high aqueous durability for underground water, and the glass sample containing CaO shows the highest durability among all samples.

On the other hand, it can be observed also that for glasses containing BaO, SrO, CaO there is little significant change in DR with increasing the immersion periods. The higher Ca, Sr and Ba content the higher is the aqueous durability of the glass, that is, the introduced Ca, Sr or Ba oxides into iron phosphate network improves their resistance against underground water (especially the sample containing 15 mol% CaO). The gradual decrease of the dissolution rate and hence the gradual increase of durability with the gradual increase of the introduced oxides (CaO, SrO, BaO) may be due to the formation some cross-linking bonds and the formation of some bonds of the form P-O-Ca, P-O-Sr or P- O- Ba.

Also, it is found that the lowest dissolution rate, that is the highest aqueous durability against underground water, is exhibited by the sample containing 15 mol% CaO,. This can be supposed to be due to the high cross-linking density and the formation of some Ca-O-Fe bonds. Such bonds are characterized by their high bond energy and small bond length [40].

Table 1. The change of DR as a function of CaO content.

x (mol%)	Log DR 6 h	Log DR 12 h	Log DR 24 h	Log DR 48 h
5	0.49	0.516	0.571	0.608
10	0.094	0.0992	0.10612	0.108
15	0.017	0.018	0.019	0.0199

Table 2. The change of DR as a function of SrO content.

x (mol%)	Log DR 6 h	Log DR 12 h	Log DR 24 h	Log DR 48 h
5	0.599	0.66	0.719	0.801
10	0.092	0.0982	0.10712	0.158
15	0.014	0.015	0.016	0.0169

Table 3. The change of DR as a function of BaO content.

x (mol%)	Log DR 6 h	Log DR 12 h	Log DR 24 h	Log DR 48 h
5	0.61	0.68	0.79	0.891
10	0.231	0.24	0029	0.316
15	0.0164	0.017	0.018	0.019

3.6. Micro hardness measurements

Surface hardness is the resistance to the localized indentations of the surface by an indenter. The load applied to the surface of the material results in both plastic and elastic deformation of the surface.

The study of the micro-hardness properties of the glasses that can be used as γ-ray shielding materials and/or to capsulate the radio-active wastes are important. These studies will determine approximately the degree of cracking that may occur due to the bearing load when interment underground.

The variation of the hardness *(H)* with the gradual increase of CaO, SrO or BaO, are exhibited in Table (4). It can be seen that the hardness increased as CaO, SrO or BaO were gradually increased and that the hardness of the glass that contains 15 mol% CaO represents the highest value in comparison with those containing SrO or BaO. The observed increase in *H* is related to the increase of the rigidity of glass and these results are found in consistent with those obtained from aqueous durability results. Also the existence Ca caions in the interstitial position through the glass network make it harder than those containing Sr or Ba cations. This may be due to the high cross linking density obtained by Ca cations, since such cations represent the lighter and smaller one in comparison to Sr or Ba cations, knowing that Ca-O bonds are of small length and high energy [25-37].

Table 4. The hardness values as a function of the introduced oxides (CaO, SrO or BaO).

Mol.%	H_V
5 % CaO	662.74
10 % CaO	729.94
15 % CaO	804.55
5 % SrO	659.93
10 % SrO	687.54
15 % SrO	722.56
5 % BaO	579.59
10 % BaO	641.757
15 % BaO	698.923

4. Conclusion

According to the studies performed on the prepared glasses, it can be concluded that the glass containing 15 mol % CaO represented the highest hardness and aqueous durability value against underground water. The glass containing 15 mol % BaO represents the best sample that can be used as ɤ-ray shielding, where it shows the highest gamma – ray mass attenuation coefficient and the lowest *HVL*. Such sample represents also the highest density and molar volume values. In addition, it shows also a good level of hardness and aqueous durability. However, it can be recommended that such samples can be used as a transparent gamma ray shield and to capsulate the radioactive wastes before interment underground.

Corresponding Author:
Prof. Dr. Ahmed G. Mostafa
ME Lab., Phys. Dept.
Faculty of Science,
Al-Azhar Univ., Nasr City, Cairo, Egypt
E-mail: *drahmedgamal@yahoo.com

References

1. C. K. Loong, K. Suzuya, D. L. Price, B.C. Sales and L. A. Boatner, Physica (B) Condensed Matter, 241 (1997) 890.
2. S.W. Martin, European Journal of Solid State and Inorganic Chemistry, 28 (1991) 164.
3. G. Little Flower, M. Srinivasa Reddy, G. Sahaya Baskaran and N. Veeraiah, Opt. Materials, 30 (2007) 357.
4. R.C. Ropp, Molecules, 15 (1992) 321.
5. U. Hoppe, J. Non-Cryst. Solids, 196 (1996) 138.
6. R. K. Brow, D. R. Tallant, Z. A. Osborne, Y. Yang and D. E. Day, Phys. Chem. Glasses, 32 (1991) 188.
7. G. C. Bhar, U. Chatterjee, A. M. Rudra and A. K. Chaudhary, J. Phys. (D) Appl. Phys., 30 (1997) 2693.

8. H. S. Liu and T. S. Chin, Phys. Chem. Glasses, 38 (1997) 123.
9. Y. Keun Lee and S. H. Choi, J. Korean Acad. Periodical, 38 (2008) 273.
10. R. K. Brow, J. Non-Cryst. Solids, 263 (2001) 1.
11. B. C. Sales and L. A. Boatner, Science, 226 (1984) 45.
12. B. C. Sales and L. A. Boatner, J. Am. Ceram. Soc., 70 (1987) 615.
13. A. Ghosh, J. Appl. Phys., 64 (1988) 2652.
14. D. E. Day, Z. Wu., C. S. Ray and P. R. Hrma, J. Non-cryst. Solids, 241 (1998) 1.
15. J. Livage, J. P. Jollivet and E. Tronc, J. Non-Cryst. Solids, 121 (1990) 35.
16. Y. Sakurai, J. Yamaki and J. Electrochem. Soc., 32 (1985) 512.
17. F. H. El Batal, A. M. Abdelghany and R. L. Elwan, J. molecular structure, 1000 (2011) 103.
18. A. K. Varshneya,"*Fundamentals of Inorganic Glasses*," Society of Glass Technology, Sheffield, UK (2006).
19. A.G. Mostafa, M.Y. Hassaan, A.B. Ramadan, A.Z. Hussein and A.Y. Abdel-Haseib, Nature and Science, 5 (2013) 11.
20. A.G. Mostafa, Turk. J. Phys., 26 (2002) 441.
21. Sukhpal Singh, Ashok Kumar, Devinder Singh, Kulwant Singh Thind,Gurmel and S. Mudahar, , Nuclear Instruments and Methods in Physics Research(B), 266 (2008) 140.
22. Murat Kurudirek, ibrahim Tu rkmen and Yuksel zdemir, Radiation Physics and Chemistry, 78 (2009) 751.
23. S. Tuscharoen, J. Kaewkhao, P. Limkitjaroenporn, P. Limsuwan and W. Chewpraditkul, Annals of Nuclear Energy, 49 (2012) 109.
24. S. N. Salama, H. Darwish and H. A. Abo-Mosallam, Ceram. Inter., 32 (2006) 357.
25. Heba A. Saudi, Sawsan El Mosallamy, Samir U. El Kameesy, Nashwa Sheta, Ahmed G. Mostafa, Hanaa A. Sallam, *World Journal of Condensed Matter Physics*, 3 (2013) 9.
26. I. Hana and L. Demirb, Journal of X-Ray Science and Technology, 18 (2010) 39.
27. A. G. shikerkar, J. A. E. Desa, P. S. R. Krishna and R. Chitra, J. Non-Cryst. Solids, 270 (2000) 234.
28. J. C. Buyn, B. H. Kim, K. S. Hong, H. J. Jung, S. W. Lee and A. A. Lzyneev, J. Non-Cryst. Solids, 190 (1995) 288.
29. L. Baia, D. Muresan, M. Baia, J. Popp and S.Simon, Vib. Spectrosc. 43 (2007) 313.
30. S. N. Salman and H. A. El-Batal, J. Non-Cryst. Solids, 168 (1994) 179.
31. S. A. MacDonald, C. R. Schardt, D. J. Masiello and J. H. Simmons, J. Non-Cryst. Solids, 275 (2000) 72.
32. A. A. Akatov, B. S. Nikonov, B. I. Omelyanenko, S. V. Stefanovsky and J. C. Marra, Phys. Chem. Glasses, 35 (2009) 245.
33. M. S. Aziz, F. Abdel-Wahab, A. G. Mostafa and E. M. El Agwany, J. Mater. Chem. Phys., 91 (2005) 532.
34. A. M. Abdel-Ghany, A. A. Bendary, T. Z. Abou-Elnasr, M.Y. Hassaan and A.G. Mostafa, Nature and Science, 12 (2014) 6.
35. A. M. Efimov, J. Non- Cryst. Solids, 209 (1997) 209.
36. A. G. Mostafa, M. A. Salem and Z. A. El-Hadi, J. Mater. Science & Technology, 18 (5) (2002) 391.
37. A. A. Ramadan, A. G. Mostafa, M. Y. Hassaan, A. Z. Hussein and A. Y. Abdel-Haseib, Isotope & Rad. Res., 46 (1) (2014) 83.
38. G. S. M. Ahmed, A. S. Mahmoud, S. M. Salem and T. Z. Abou-Elnasr, American J. Phys. & Application, 3 (4) (2015) 112.
39. H. Mori, H. Matsuno and H. Sakata, J. Non-Cryst Solids, 276 (2000) 78.
40. M. Karabulut**,** B. Yuce**,** O. Bozdogan**,** H. Ertap and G.M. Mammadov, J. Non-Cryst. Solids, 5 (2011) 1455.

11/25/2015